

Clinical Relevance of Single-Voxel ¹H MRS Metabolites in Discriminating Suprasellar Tumors

A EINSTIEN¹, RAHUL A VIRANI²

ABSTRACT

Introduction: Spatially resolved metabolic data obtained from Proton Magnetic Resonance Spectroscopy (¹H MRS) provides information which increases the diagnostic accuracy of imaging sequences in predicting the histology of suprasellar tumors.

Aim: To evaluate the role of ¹H MRS in the diagnosis of various suprasellar tumors.

Materials and Methods: Sixty cases of various suprasellar, hypothalamic and third ventricular neoplasms were investigated with long-echo single voxel ¹H -MRS using 1.5 Tesla clinical imager. Single-voxel spectroscopic examinations were guided by T1-weighted or T2-weighted images. Statistical analysis was carried out using IBM SPSS software version 19.

Results: We observed that whenever brain tissue was damaged

or replaced by any process, NAA was markedly reduced. Extra-axial lesions which do not infiltrate brain or contain neuroglial tissue, didn't demonstrate any NAA resonances. Cr was used as an internal standard for semi-quantitative evaluation of metabolic changes of other brain metabolites. Increased Cho was seen in processes with elevated cell-membrane turnover.

Conclusion: Spectra obtained from different tumors exhibit reproducible differences while histologically similar tumors yield characteristic spectra with only minor differences. Pituitary tumors were typically characterized by significant reduction of NAA, Cr peak and moderate elevation of Cho peak. Gliomas were typically characterized by decrease of NAA and Cr peaks and increase of Cho peak. Craniopharyngiomas were typically characterized by significant decrease of all metabolites.

Keywords: Choline, Creatine, N-acetylaspartate, Spectroscopy

INTRODUCTION

In neurosurgical practice suprasellar tumors are very common. Pituitary adenomas, craniopharyngiomas, meningiomas and gliomas are generally the most frequent tumors in this area, but the whole spectrum of the possible pathologies is extremely wide, and includes both neoplastic and non-neoplastic masses. In many cases, these different entities can be readily distinguished by MRI alone or by MRI in combination with computed tomography, [1]. But even after using the most up-to-date equipment and imaging sequences, a definitive histological diagnosis often cannot be made preoperatively [2].

Proton Magnetic Resonance Spectroscopy (¹H MRS) is widely available as a software upgrade to MRI imaging equipment. Spatially resolved metabolic data obtained from ¹H MRS provides information which increases the diagnostic accuracy of imaging sequences in predicting the histology of suprasellar neoplasms [3,4]. MR spectroscopy and DWMRI are considered important diagnostic tools complementary to cMRI in pre-surgical evaluation and discrimination between different sellar and suprasellar lesions [4].

AIM

To evaluate the role of ¹H spectroscopy in the diagnosis of various suprasellar, hypothalamic and third ventricular neoplasms. To categorize different suprasellar tumors using their pathological ¹H spectroscopic characteristics according to the classification by Chernov et al., [5].

MATERIALS AND METHODS

This prospective study was carried out in the Department of Radiodiagnosis of SMS hospital between October 2010 through September 2012 and Chettinad Hospital and Research Institute and in Department of Radiology in Chettinad Hospital and Research Institute between October 2012 through September 2014. Institutional ethical approval was obtained for the study.

Sixty cases (suprasellar, hypothalamic and third ventricle tumors) among the patients who were advised MRI were investigated, with long-echo single voxel ¹H-MRS. Informed consent from the patients was received and all investigations were done using 1.5 Tesla clinical imager (General electronics Signa Excite). Single-voxel spectroscopic examinations were guided by T1-weighted or T2-weighted images and where needed, postgadolinium T1-weighted MRI was used. Under three dimensional control, the rectangular ¹H-MRS voxel was placed on the projection of the solid part of the tumor with avoidance of its cystic/ necrotic areas, as well as contamination with skull and cerebral ventricles. Acquisition of the spectrum was by STimulated Echo Acquisition Mode (STEAM). The size of the voxel used was either 15 x 15 x 15 mm (volume: 3.4 cc), or 20 x 20 x 20 mm (volume: 8 cc).

Metabolite signals from mobile lipids (Lip), lactate (Lac), N-acetylaspartate (NAA), creatine (Cr), and choline-containing compounds (Cho), centered, respectively at 0.9, 1.3, 2.0, 3.0, and 3.2 ppm, were obtained. Presence of each metabolite peak was initially evaluated qualitatively by visual inspection and type of the pathological ¹H-MR spectra was determined according to the classification as in [Table/Fig-1]. Additionally, the content of NAA, Cho, and Cr in tumors was expressed relatively to their corresponding metabolites in the reference spectrum of the normal brain tissue (Mtbumor/Mtbbrain). Peak intensity of NAA, Cho and Lip were normalized to Cr of the normal brain (nCr), and ratio Lip/NAA was calculated. Statistical analyses were done using IBM SPSS software version 19.

Our study included 34 males and 26 females, aged between 6 and 71 years with a median age of 31 years. There were 28 pituitary adenomas, 12 gliomas, 8 craniopharyngiomas, 4 chordomas, 2 each of meningiomas, malignant lymphomas, Rathke cleft cysts and 1 each of germinoma, hypothalamic hamartoma. The MRS metabolites of 4 commonly encountered lesions viz. pituitary adenoma, glioma, craniopharyngioma and chordoma were identified, quantified and tabulated. Metabolites of occasionally confronted lesions were dealt with independently.

RESULTS

The present data from our study has shown that in initially diagnosed tumors with large suprasellar extension ¹H-MRS can provide valuable metabolic information. The various pathological ¹H-MR spectra are categorized and typed based on [Table/Fig-1]. The observed NAA content, Cho content and Cr content of four major suprasellar tumors namely pituitary adenoma, glioma, craniopharyngioma and chordoma are quantified in [Table/Fig-2-4], respectively. ¹H-MR spectra of the pituitary tumors in the study were typically characterized by significant reduction of NAA peak, moderate elevation of Cho and infrequent presence of small Lip and Lac peaks [Table/Fig-5,6]. nCr level was found to be constant and various ratios Lip/nCr*, NAA/nCr*, Cho/nCr* were calculated [Table/Fig-7-9].

Pituitary Adenomas

Among 28 tumors, 17 were functional and rest non-functional. ¹H-MR spectra of the pituitary tumors were typically characterized by significant reduction of NAA peak, which was not identified at all in 14 cases, absence (8 cases) or presence of only residual (6 cases) Cr peak, moderate elevation of Cho and infrequent presence of small Lip and Lac peaks. Seven cases had type I A spectra, 3 cases had type II B spectra, 5 cases had type II C with mild elevation of lip peak, 4 cases had type II C with moderate elevation of lip peak, 3 cases had type III C while 6 cases had type IIIB. It should be noted, that even in cases with moderate elevation of Lip, increase of Lip/NAA ratio above 1 was seemingly caused not by elevation of the Lip content, but by significant decrease of NAA [Table/Fig-10,11]. No significant differences were found between functional and non-functional tumors.

Gliomas

Among 12 gliomas there were 7 WHO Grade I tumors while 5 were WHO Grade II tumors. ¹H-MR spectra of gliomas were typically characterized by decrease of NAA and Cr peaks, and increase of Cho peak, which, however, were usually preserved [Table/Fig-12]. Lip and Lac peaks were identified in 4 and 5 cases, respectively. Ten tumors had pathological ¹H-MR spectra Type II: 4—Type II A, 3—Type II B, and 3—Type II C with moderate elevation of Lip. Two tumors had type III C spectra. Identification of NAA in gliomas can be caused either by infiltrative growth of the tumor and presence of viable neurons within the bulk of neoplasm or by production of the metabolite by the neoplastic cells itself [6].

| Type of the pathological ¹ H-MR spectra | Predominant metabolite Peak | Presence of Lac peak | Presence of Lip peaks |
|--|--|----------------------|-----------------------|
| Type I A | NAA (NAA content<0.75 and/or Cho content>1.25) | No | No |
| Type I B | NAA | Yes | No |
| Type I C with mild elevation of Lip | NAA | Not relevant | Yes (Lip/Cho<1) |
| Type I C with moderate elevation of Lip | NAA | Not relevant | Yes (Lip/Cho>1) |
| Type II A | Cho | No | No |
| Type II B | Cho | Yes | No |
| Type II C with mild elevation of Lip | Cho | Not relevant | Yes (Lip/NAA<1) |
| Type II C with moderate elevation of Lip | Cho | Not relevant | Yes (Lip/NAA>1) |
| Type III A | Lip (Cho peak preserved) | Not relevant | Yes |
| Type III B | Lip (significant reduction or disappearance of Cho peak) | Not relevant | Yes |
| Type III C | Absence of any detectable peak | | |

[Table/Fig-1]: Types of the pathological ¹H-MR spectra [5].

Craniopharyngiomas

¹H-MR spectra of the tumors were typically characterized by significant decrease of all metabolites and presence of multiple additional peaks [Table/Fig-13]. Two tumors had pathological ¹H-MR spectrum Type II C with mild elevation of Lip, whereas 6 others had pathological ¹H-MR spectra Type III C.

Chordomas

¹H-MR spectra of the tumors were typically characterized by significant decrease of NAA and Cr peaks, and profound elevation of Cho and Lip peaks [Table/Fig-14]. Prominent Lac peak was presented in 3 cases. All tumors had pathological ¹H-MR spectra Type II C with moderate elevation of Lip.

| Metabolic characteristics | Pituitary adenomas (28) | Gliomas (12) | Craniopharyngiomas (8) | Chordomas (4) | Statistics [†] |
|---------------------------|-------------------------|------------------|------------------------|---------------|-------------------------|
| NAA content* | 0.77 (0.39-1.22) | 0.76 (0.64-0.77) | 0.75 | 0.76 | H=0.275 (p>0.2) |

[Table/Fig-2]: NAA content*

* Data presented as medians with 95% confidence interval in parenthesis

† According to Kruskal–Wallis test

NAA-N-acetylaspartate

| Metabolic characteristics | Pituitary adenomas (28) | Gliomas (12) | Craniopharyngiomas (8) | Chordomas (4) | Statistics [†] |
|---------------------------|-------------------------|-------------------|------------------------|---------------------|-------------------------|
| Cho content* | 12.46 (2.47-14.41) | 2.55 (1.39-14.42) | 2.20 | 13.73 (13.01-14.16) | H=10.336 (p<0.05) |

[Table/Fig-3]: Cho content*

* Data presented as medians with 95% confidence interval in parenthesis

† According to Kruskal–Wallis test

Cho-choline-containing compounds

| Metabolic characteristics | Pituitary adenomas (28) | Gliomas (12) | Craniopharyngiomas (8) | Chordomas (4) | Statistics [†] |
|---------------------------|-------------------------|------------------|------------------------|---------------|-------------------------|
| Cr Content* | 0.51 (0.16-.44) | 0.46 (0.41-0.59) | NC | NC | H=0.659 (p>0.2) |

[Table/Fig-4]: Cr content*

* Data presented as medians with 95% confidence interval in parenthesis

† According to Kruskal–Wallis test

Cr-creatinine

| Metabolic characteristics | Pituitary adenomas (28) | Gliomas (12) | Craniopharyngiomas (8) | Chordomas (4) | Statistics [†] |
|---|-------------------------|--------------|------------------------|---------------|---|
| Presence of Lip 0.9 and/or Lip 1.3 peaks* | 12 | 4 | 2 | 3 | χ ² corrected =2.418 (p>0.2) |

[Table/Fig-5]: Presence of Lip0.9 and/or Lip1.3 peaks.

* Data presented as medians with 95% confidence interval in parenthesis

† According to chi-square test with continuity correction

Lip-mobile lipids

| Metabolic characteristics | Pituitary adenomas (28) | Gliomas (12) | Craniopharyngiomas (8) | Chordomas (4) | Statistics [†] |
|---------------------------|-------------------------|--------------|------------------------|---------------|---|
| Presence of Lac peak* | 10 | 5 | 1 | 3 | χ ² corrected =0.312 (p>0.2) |

[Table/Fig-6]: Presence of Lac peak.

* Data presented as medians with 95% confidence interval in parenthesis

† According to chi-square test with continuity correction

Lac-lactate

| Metabolic characteristics | Pituitary adenomas (28) | Gliomas (12) | Craniopharyngiomas (8) | Chordomas (4) | Statistics [†] |
|---------------------------|-------------------------|--------------------|------------------------|--------------------|-------------------------|
| Lip/nCr* | 7.99 (2.52-13.54) | 10.43 (92.5-12.51) | 2.76 | 13.75 (12.9-14.19) | H=6.871 (p<0.1) |

[Table/Fig-7]: Lip/nCr*

* Data presented as medians with 95% confidence interval in parenthesis

† According to Kruskal–Wallis test

nCr-creatinine of the normal brain; Lip-mobile lipids

| Metabolic characteristics | Pituitary adenomas (28) | Gliomas (12) | Cranio-pharyngiomas (8) | Chordomas (4) | Statistics [†] |
|---------------------------|-------------------------|---------------------|-------------------------|---------------|-------------------------|
| NAA/nCr* | 0.48 (0.11-1.33) | 0.47 (0.08-1.98) | 1.78 | 0.34 | H=1.419 (p>0.2) |

[Table/Fig-8]: NAA/nCr*

*Data presented as medians with 95% confidence interval in parenthesis
[†] According to Kruskal–Wallis test

| Metabolic characteristics | Pituitary adenomas (28) | Gliomas (12) | Cranio-pharyngiomas (8) | Chordomas (4) | Statistics [†] |
|---------------------------|-------------------------|-----------------------|-------------------------|------------------------|-------------------------|
| Cho/nCr* | 11.62 (2.41-13.57) | 12.43 (2.51-13.56) | 0.89 | 13.74 (13.31-14.16) | H=8.421 (p<0.05) |

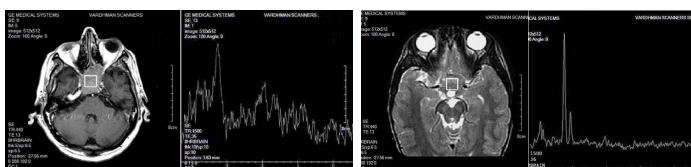
[Table/Fig-9]: Cho/nCr*

*Data presented as medians with 95% confidence interval in parenthesis
[†] According to Kruskal–Wallis test

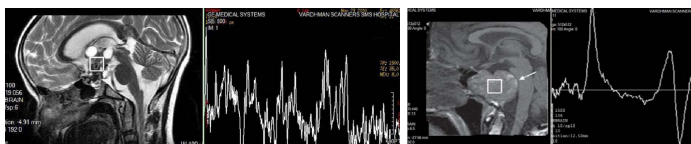
| Metabolic characteristics | Pituitary adenomas (28) | Gliomas (12) | Cranio-pharyngiomas (8) | Chordomas (4) | Statistics [†] |
|---------------------------|-------------------------|------------------------|-------------------------|---------------|-------------------------|
| Lip/NAA* | 21.29 (2.16-25.49) | 27.12 (24.16-29.12) | 5.75 | 31.03 | H=5.233 (p>0.2) |

[Table/Fig-10]: Lip/NAA*

*Data presented as medians with 95% confidence interval in parenthesis
[†] According to Kruskal–Wallis test
 NC - not calculated

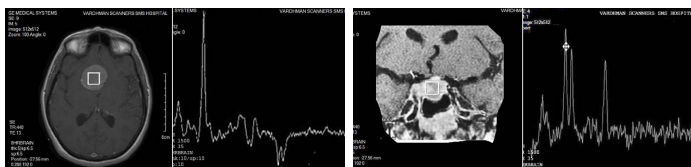


[Table/Fig-11]: PITUITARY ADENOMA: Spectroscopy of a pituitary adenoma shows significant reduction of NAA peak, Cr peak, moderate elevation of Cho, and a small Lip and Lac peak. [Table/Fig-12]: GLIOMA: Spectroscopy of a glioma shows decrease of NAA and Cr peaks and increase of Cho peak and a small Lip and Lac peak.



[Table/Fig-13]: CRANIOPHARYNGIOMA: Spectroscopy shows significant decrease of all metabolites and presence of multiple additional peaks.

[Table/Fig-14]: CHORDOMA: Spectroscopy shows significant decrease of NAA and Cr peaks and profound elevation of Cho and Lip peaks and the presence of lactate peak.



[Table/Fig-15]: MENINGIOMA: Spectroscopy shows mild elevation of Lip, absence of NAA peak, residual Cr peak, mild elevation of Cho, presence of small Lac and Lip peaks as well as an alanine peak. [Table/Fig-16]: LYMPHOMA: Spectroscopy shows moderate elevation of Lip, decrease of NAA peak, residual Cr peak, slightly increased Cho peak, and presence of a Lac and Lip peak.

Others

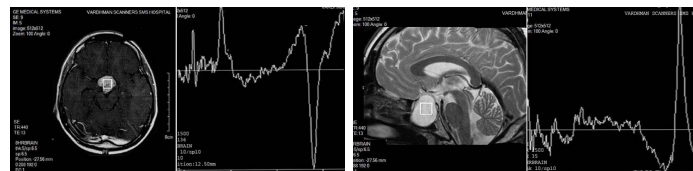
Both meningiomas had pathological ¹H-MR spectrum Type II C with mild elevation of Lip, which was characterized by absence of NAA peak, residual Cr peak, mild elevation of Cho, presence of small Lac and Lip peaks [Table/Fig-15].

Malignant lymphoma (two cases) had pathological ¹H-MR spectrum Type II C with moderate elevation of Lip, which were characterized by decrease of NAA peak, residual Cr peak, slightly increased Cho peak and presence of Lac and Lip peaks [Table/Fig-16].

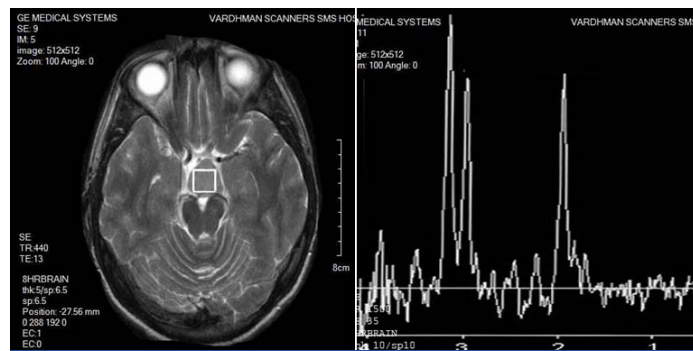
Germinoma had pathological ¹H-MR spectrum Type II C with moderate elevation of Lip, which was characterized by absence of NAA peak, residual Cr peak, significant elevation of Cho peak, and presence of prominent Lip and Lac peaks [Table/Fig-17].

Rathke's cleft cyst (two cases) had pathological ¹H-MR spectrum Type III B, which were characterized by absence of any metabolite peaks beside Lip and Lac [Table/Fig-18].

Hypothalamic hamartoma had pathological ¹H-MR spectrum Type II A, which was characterized by decrease of NAA peak, practically unchanged Cr peak, and slightly increased Cho peak [Table/Fig-19].



[Table/Fig-17]: GERMINOMA: Spectroscopy shows moderate elevation of Lip, absence of NAA peak, residual Cr peak, significant elevation of Cho peak, and presence of prominent Lip and Lac peaks. [Table/Fig-18]: RATHKE'S CLEFT CYST: Spectroscopy is characterized by absence of any metabolite peaks beside Lip and Lac.



[Table/Fig-19]: HYPOTHALAMIC HAMARTOMA: Spectroscopy is characterized by decrease of NAA peak, practically unchanged Cr peak, and slightly increased Cho peak.

DISCUSSION

Magnetic Resonance Imaging (MRI) is now a widely accepted modality for delineating normal and pathological structures within the brain. Discrimination among different types of pathological tissues remains difficult and in cases of brain tumors, biopsy is often required to establish a specific pathological diagnosis. Proton magnetic resonance spectroscopy (¹H-MRS) gives completely different information related to neuronal integrity, cell proliferation or degradation, energy metabolism, and necrotic transformation of brain or tumour tissues [7,8]. In conjunction with structural imaging modalities, ¹H-MRS plays an increasingly important role in a number of common neurological disorders [9,10] and MRS may be useful in providing a more improved preoperative diagnosis of suprasellar tumors [11].

In spite of the fact that the function of NAA is not known exactly, it is generally recognized as a marker of functional neurons and their appendages (including dendrites). Whenever brain tissue is damaged or replaced by any destructive, degenerative or infiltrative process, NAA is markedly reduced [12-14]. This is in concordance with the results of the study. Extra-axial lesions, which do not infiltrate brain or which do not contain neuroglial tissue, will not demonstrate any NAA resonances. Since Cr-bound phosphates are a substrate of the ATP/ADP cycle, Cr is considered to be an indicator of energy metabolism. Cr is quite constant in various metabolic conditions, it has often been used as an internal standard for semi-quantitative evaluation of metabolic changes of other brain metabolites—Cho resonances originate mainly from intermediates of phospholipid metabolism such as phosphocholine and glycerophosphocholine, which both play an important role in the structure and function of cell membranes. Consequently, increased Cho can be seen in processes

with elevated cell-membrane turnover, such as in proliferating tumors [12-14]. In the present study, pituitary adenomas and chordomas showed significant increase in Cho content. Lipids and lactate are physiologically not detectable in healthy brain. In-vitro studies have shown that the amount of lipids detected by spectroscopy correlates well with the degree of micro- and macronecrosis seen on histology. Brain lactate is produced in conditions of anaerobic glycolysis, i.e. during a mismatch between glycolysis and oxygen supply and indicates hypoxic conditions as well as hypermetabolic glucose consumption [15].

¹H MRS permits exact spatial localization and interpretable spectra may be obtained from regions of interest as small as 8 cm³, thus allowing data to be obtained from relatively small tumors. Unfortunately, metabolites cannot be readily quantified in terms of absolute concentrations and data must be expressed in terms of the ratios of the different peaks. Nevertheless, metabolites may be measured noninvasively and repetitively in a manner not possible by other methods [16].

CONCLUSION

MRS findings should never be used in isolation but interpreted in conjunction with the clinical and spatial imaging findings. This is especially important if the list of possible pathologies for differential diagnosis is as wide as in suprasellar region. As it is shown in the present series there is definite variation of the metabolic patterns in neoplasms with the same histological type, whereas more or less similar neurochemical alterations can be observed in completely different diseases. However, there is clear evidence that spectra obtained from different tumors exhibited reproducible differences, while histologically similar tumors yielded characteristic spectra with only minor differences.

REFERENCES

- [1] Rennert J, Doerfler A. Imaging of sellar and parasellar lesions. *Clin Neurol Neurosurg.* 2007;109(2):111-24.
- [2] Julia-Sape M, Acosta D, Majos C, Moreno-Torres A, Wesseling P, Acebes JJ, et al. Comparison between neuroimaging classifications and histopathological diagnoses using an international multicenter brain tumor magnetic resonance imaging database. *J Neurosurg.* 2006;105(1):6-14.
- [3] Chaudhary V, Bano S. Imaging of the pituitary: Recent advances. *Indian J Endocrinol Metab.* 2011; 15(Suppl3): S216-S23.
- [4] Mohammada FF, Hasana DI, Ammarb MG. MR spectroscopy and diffusion MR imaging in characterization of common sellar and supra-sellar neoplastic lesions. *The Egyptian Journal of Radiology and Nuclear Medicine.* 45(3), 2014, 859-67.
- [5] Chernov MF, Takakazu K, Kosaku A, Ono Y, Suzek T, et al. Possible role of single-voxel ¹H-MRS in differential diagnosis of suprasellar tumors. *J Neurocol.* 2009;91:191-98.
- [6] Chernov MF, Ono Y, Kubo O, Hori T. Comparison of ¹H-MRS-detected metabolic characteristics in single metastatic brain tumors of different origin. *Brain Tumor Pathol.* 2006;23(1):35-40.
- [7] Kwock L, Smith JK, Castillo M, Ewend MG, Cush S, Hensing T, et al. Clinical applications of proton MR spectroscopy in oncology. *Technol Cancer Res Treat.* 2002; 1: 17-28.
- [8] Lin G, Chung YL. Current opportunities and challenges of magnetic resonance spectroscopy, positron emission tomography, and mass spectrometry imaging for mapping cancer metabolism in vivo. *Bio Med Research International.* Volume 2014 (2014), Article ID 625095.
- [9] Möller-Hartmann W, Herminghaus S, Krings T, Marquardt G, Lanfermann H, Pilatus U, et al. Clinical application of proton magnetic resonance spectroscopy in the diagnosis of intracranial mass lesions. *Neuroradiology.* 2002;44:371-81.
- [10] Lee PL, Gonzalez RG. Magnetic resonance spectroscopy of brain tumours. *Curr Opin Oncol.* 2009 1; 2(4): 271-80.
- [11] Jouibari MF, Ghodsi SM, Akhlaghpour S et al. Complementary effect of H-MRS in diagnosis of suprasellar tumors. *Clinical Imaging.* 2012; 36(6): 810 - 15.
- [12] Falini A, Calabrese G, Origgi D, Lipari S, Triulzi F, Losa M, et al. Proton magnetic resonance spectroscopy and intracranial tumours: clinical perspectives. *J Neurol.* 1996;243:706-14.
- [13] Amstutz DR, Coons SW, Kerrigan JF, Rekeate HL, Heiserman JE. Hypothalamic hamartomas: Correlation of MR imaging and spectroscopic findings with tumor glial content. *AJNR Am J Neuroradiol.* 2006;27(4):794-98.
- [14] Horská A, Barker PB. Imaging of brain tumors: mr spectroscopy and metabolic imaging neuroimaging. *Clin N Am.* 2010; 20(3): 293-310.
- [15] Kim JP, Lentz MR, Westmoreland SV, et al. Relationships between astrogliosis and ¹H MR spectroscopic measures of brain choline/creatine and myo-inositol/creatine in a primate model. *AJNR Am J Neuroradiol.* 2005;26:752-59.
- [16] Bruhn H, Frahm J, Gyngell M, Merboldt KO, Hanicke W, Sauter R, et al. Noninvasive differentiation of tumors with use of localized H1 MR spectroscopy in vivo: Initial experience in patients with cerebral tumors. *Radiology.* 1989. 172:541-48.

PARTICULARS OF CONTRIBUTORS:

1. Assistant Professor, Department of Radiology, Chettinad Hospital & Research Institute, Kelambakkam, Tamil Nadu, India.
2. Consultant, Department of Radiology, Horizon Imaging, Morbi, Rajkot, Gujarat, India.

NAME, ADDRESS, E-MAIL ID OF THE CORRESPONDING AUTHOR:

Dr. A. Einstien,
Assistant Professor, Department of Radiology, Chettinad Hospital & Research Institute,
Rajiv Gandhi Salai, Kelambakkam, Tamil Nadu - 603103, India.
E-mail: einstien.raj@ gmail.com

FINANCIAL OR OTHER COMPETING INTERESTS: None.

Date of Submission: **Nov 27, 2015**
Date of Peer Review: **Dec 11, 2015**
Date of Acceptance: **Jan 08, 2016**
Date of Publishing: **Jul 01, 2016**